

Phase States and Structural, Jahn–Teller, and Magnetic Transitions in Weakly Doped Lanthanum–Strontium Manganites

V. A. Golenishchev-Kutuzov^a, A. V. Golenishchev-Kutuzov^{a,*}, R. I. Kalimullin^a, and A. V. Semennikov^a

^aKazan State Power Engineering University, Kazan, 420066 Russia

*e-mail: campoce6e@gmail.com

Received November 20, 2018; revised December 16, 2018; accepted February 25, 2019

Abstract—A phase diagram describing the structural, magnetic, transport, and Jahn–Teller properties and their interrelation as a function of the composition and temperature is constructed using the results from measuring elastic moduli, electrical conductivity, and magnetization for lanthanum–strontium manganites of the form $\text{La}_{1-x}\text{Sr}_x\text{MnO}_3$ ($0.165 \leq x \leq 0.18$). Local and cooperative Jahn–Teller distortions of the structural MnO_6 octahedra and their effect on the physical properties of materials are studied.

DOI: 10.3103/S1062873819060169

INTRODUCTION

The unusual physical properties of weakly doped manganites of the $\text{La}_{1-x}\text{Sr}_x\text{MnO}_3$ type ($0.10 \leq x \leq 0.20$) have been the object of numerous studies for more than two decades, due to the variety of their structural and magnetic states, electrical conductivity, the observed colossal magnetoresistance (CMR) effect, and the possibilities of practical application. A phase diagram of their structural, electrical, and magnetic states versus composition (x) is shown in Fig. 1. It is now obvious that the nature of these effects is cannot be explained without considering the Jahn–Teller (J–T) distortion of the MnO_6 octahedra and different types of their structural ordering. If in the past it was mainly the cooperative ordering of MnO_6 that was studied, the local ordering of MnO_6 in the form of nanoscale clusters, which apparently also affect the physical properties of manganites, has now been established. Of greatest interest are lanthanum–strontium manganites with composition $0.165 \leq x \leq 0.18$, which has the strongest colossal magnetoresistance. Its phase diagram (x, T) shows the intersection of the curves for the paramagnet–ferromagnet (T_C) phase transition, the transition from isolator to metallic conductivity (I–M), the structural phase transition (T_S) from the rhombohedral to the orthorhombic phase (R–O), and striction. It has recently been noted that different types of X-ray, electron, and neutron diffraction are most effective for studying features of the J–T effect in manganites [1, 2]. However, their resolution is sufficient only for studying either individual structural elements (MnO_6) or their cooperative ordering. They are less suitable for the local ordering of J–T distorted MnO_6 up to 100 \AA , due to the smearing of diffraction

signals [2]. The J–T ordering of MnO_6 has thus been studied only for non-doped LaMnO_3 samples. Using theoretical simulations of experimental results, a model has now been developed for the temperature variation of the cooperative and local ordering of J–T distorted MnO_6 octahedra [3, 4].

For such studies of the J–T effect in weakly doped manganites, we have developed and tested a complex

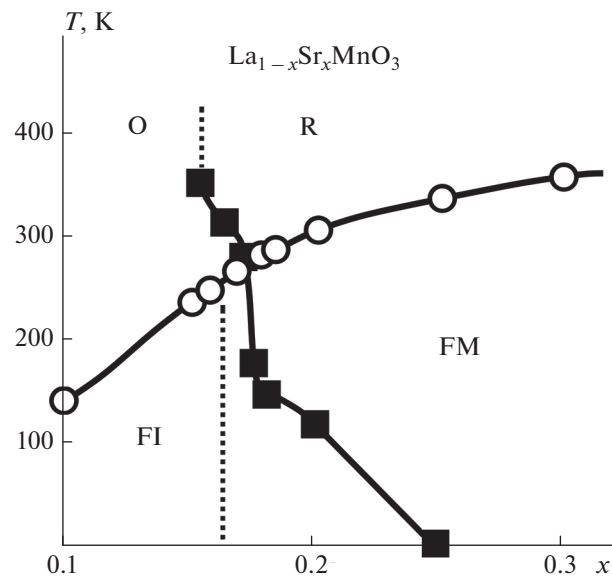


Fig. 1. Temperatures of the structural (T_S) and magnetic (T_C) transitions for the rhombohedral (R) and orthorhombic (O) states in the magnetodielectric (FI) and ferromagnetic metallic (FM) phases, depending on the composition of $\text{La}_{1-x}\text{Sr}_x\text{MnO}_3$ ($0.1 \leq x \leq 0.3$).

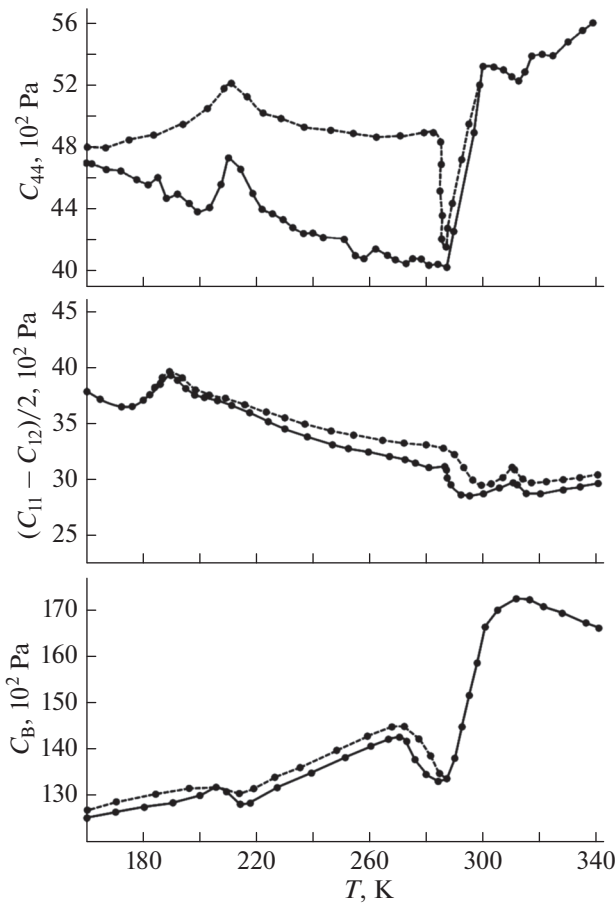


Fig. 2. Temperature dependences of the elastic moduli for our $\text{La}_{1-x}\text{Sr}_x\text{MnO}_3$ ($x = 0.175$) sample. $H = 0$, solid lines; $H = 1.5$ T, dashed lines.

procedure that includes high-frequency (up to 1000 MHz) acoustic spectroscopy, and magnetic and resistive measurements (400–140 K) [5, 6]. Based on the technique described in [6] for determining the nature of the MnO_6 ordering from the change of the Mn–O bond lengths and the Mn–O–Mn bond angles, we have developed a way of estimating these parameters from the measured temperature and magnetic changes in a set of elastic moduli C_{ij} . The $(C_{11} - C_{12})/2$ value characterizes the change in Mn–O bond lengths caused by transverse deformation C_{ij} , the change in C_{44} corresponds to the deviation of the bond angles from 180° , and bulk module C_B reflects the change in the volume of the sample during cooperative ordering. The changes in bond lengths during J–T transitions were determined from the corresponding deformations (e) proportional to the softening of C_{ij} .

Based on measurements of the temperature and field dependences of the C_{11} , $(C_{11} - C_{12})/2$, C_{44} , and C_B moduli at field strengths of up to 1.5 T, using the model of J–T ordering for LaMnO_3 , and analyzing earlier acoustic measurements made at low frequen-

cies (1–10 MHz) for similar manganite samples [7], we arrived at certain conclusions and assumptions that applied to a series of weakly doped $\text{La}_{1-x}\text{Sr}_x\text{MnO}_3$ ($0.165 \leq x \leq 0.18$). These referred to different types of J–T ordering and their effects on some of the physical properties of this class of manganites.

J–T distortions of individual MnO_6 octahedra occur near the high-temperature structural transition from the quasicubic (Q) to the rhombohedral (R) phase [3, 4]. The structure and degree of deformation of individual MnO_6 samples depend little on the temperature of the crystalline and magnetic states, but e falls as x rises. However, magnetic ordering competes with the local and cooperative ordering of MnO_6 octahedra. In addition, to reach the minimum internal energy, magnetic ordering reduces or even suppresses J–T ordering. Experiments have shown that in all samples with $x = 0.165, 0.17, 0.175$, and 0.180 , the values of the elastic moduli change as early as the rhombohedral (R) phase [6–10]. In addition, the occurrence of local orderings (clusters) of already J–T distorted MnO_6 octahedra was established from the character of the temperature dependences of the elastic moduli [8]. It was found that such clusters also affect the physical characteristics of the investigated manganites. The smooth reduction in the $(C_{11} - C_{12})/2$ and C_{66} moduli and the slight changes in C_{44} corresponding to those in Mn–O bond lengths and Mn–O–Mn angles in octahedra, which begin below 400 K in the rhombohedral (R) phase, can be attributed to a linear increase in the local ordering of completely distorted MnO_6 octahedra (Fig. 2). This process is logically associated with the increase in electrical resistance ρ (Fig. 3), since the increase in cluster sizes can produce additional scattering of high-frequency acoustic waves. This increase in cluster size was interrupted for samples with $x \geq 0.165$, and their number fell considerably near $T_{J-T} = 310$ K, as was confirmed by the stepwise change in most elastic moduli and the drop in ρ . Since this process in terms of temperature corresponds to the decline of spontaneous magnetization (Fig. 3), we may assume that the reduction in local ordering among MnO_6 complexes at 310 K was associated with its suppression by increased magnetic ordering among the ions. Upon an increase in the applied magnetic field, this process shifted somewhat toward higher temperatures, confirming our conclusions. The absence of changes in bulk module C_B near 310 K indicates that almost all deformations of individual octahedra were preserved. We attributed similar changes in the local ordering of distorted octahedra containing J–T ions (as in the cooperative ordering process) to a first-order phase transition of the J–T type. The local ordering near the transition in the orthorhombic phase (O) detected at lower temperatures (180–200 K) was inverse to this transition (Fig. 4).

The initial formation of local ordering among J–T distorted MnO_6 (clusters) thus began as early as phase

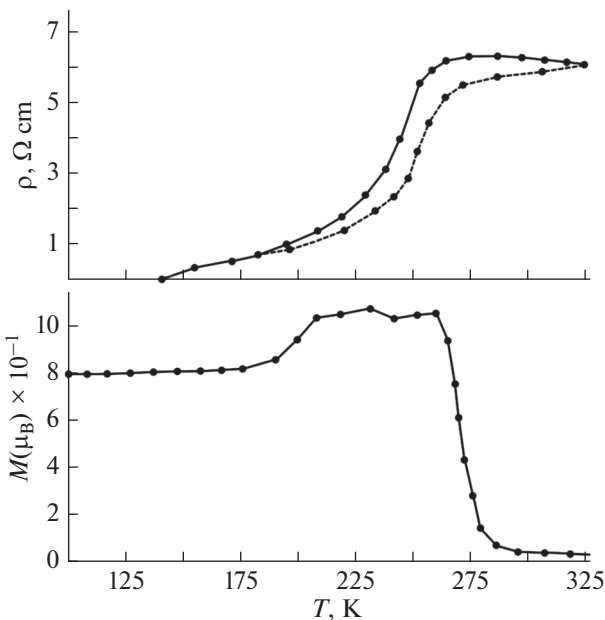


Fig. 3. Temperature dependences of specific electrical resistance ρ (at $H = 0$, solid lines; at $H = 1.5 \text{ T}$, dashed lines) and magnetization M for our sample with $x = 0.175$.

R, and the cluster sizes grew as the temperature fell. Upon the transition to orthorhombic phase O, individual clusters grew to 100 Å, but the overall size of samples remained the same. For the samples with $x \leq 0.165$ inside phase O, there was an abrupt change in all C_{ij} moduli as the temperature fell, accompanied by a substantial increase in electrical resistance ρ . These stepwise changes in C_{ij} and ρ , and their hysteresis nature, allow us to present them as a result of a first-order J–T cooperative structural phase transition with the distortion of sample shape and the transformation of clusters into a single domain. J–T cooperative ordering can therefore be attributed to independent structural phase O'. Upon a further drop in temperature, the emerging ferromagnetic ordering competes with J–T ordering and suppresses it, as is reflected in the O'–O transition. J–T transitions O–O' and O'–O both refer to the transitions of the order–disorder type; however, the first one is spontaneous and the second is a forced transition under the effect of ferromagnetic ordering. The rise in the Curie point to 277 K for the sample with $x = 0.175$ results in suppression of the J–T cooperative ordering, while elements of local ordering are preserved.

However, the most important result was detection of the stepwise, asymmetric (in terms of temperature), and intense (20–30%) change in the elastic moduli and the attenuation of acoustic waves in samples with $x = 0.17$ and 0.175 near the intersection of the structural and magnetic transitions (Fig. 1). These changes were of a hysteresis character in terms of temperature and occurred in the range of 280–300 K. The substan-

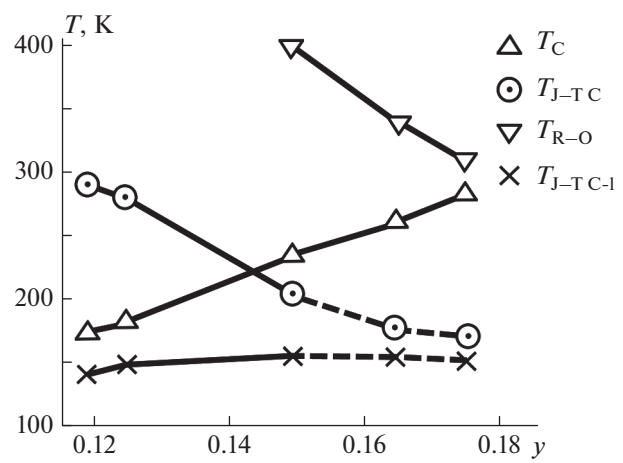


Fig. 4. Dependences of the temperatures of magnetic ordering T_C , structural transition T_{R-O} from the rhombohedral (R) to the orthorhombic (O) phase, the emergence of cooperative J–T ordering $T_{J-T C}$, and local ordering $T_{J-T C-I}$.

tial drop in the C_{44} , C_{11} moduli and the increase in $(C_{11} - C_{12})/2$ can be compared to the same abrupt change in Mn–O bond lengths and the increase in Mn–O–Mn angles, testifying to the macroscopic change in the samples with $x = 0.17$ and 0.175: the reduction along the c axis and the increase along the a and b axes. The authors of [10] reported strong striction in a sample with $x = 0.17$. Since the macroscopic size changed abruptly under conditions of an increase in magnetization and a transition to the ferromagnetic phase, we attribute it to the first-order magnetoelastic transition. In the same range of temperatures, there was simultaneously a large drop in ρ , which is typical of the transition to the ferromagnetic metal phase. Applying a magnetic field of up to 1.5 T shifted the high-temperature (280–310 K) J–T phase transitions toward lower temperatures, and the low-temperature transitions (180–200 K) upward. This can be explained by the interconnected magnetic ordering of the electron spins of Mn^{3+} ions and the change in the character of the lattice degrees of freedom for the J–T octahedra. This was confirmed by the stretching of the low-temperature structural transition T_{R-C} by tens of degrees in the samples with $x = 0.17$ and 0.175.

CONCLUSIONS

As it grows, ferromagnetic ordering results in competition with both cooperative and local ordering, and partially or completely suppresses them during the transition to the metal phase. The features of local and cooperative J–T ordering are in turn determined by the character of the orbital and magnetic orderings. Applying a strong magnetic field also suppresses local ordering, and the set of temperature characteristics of

J–T and magnetic phases favors the proposed CMR mechanism: the suppression of local J–T ordering by the external field under the conditions of spontaneous ferromagnetic ordering.

Analysis of our results showed that such forms of J–T transitions, which differ from conventional structural transitions of the R–O type by their asymmetry, narrow range of temperatures, considerable (up to 30%) change in C_{ij} , and the strong effect of the magnetic fields, are characteristic only of narrow sample compositions where T_C and T_S are separated by as much as 30 K. These features of samples with $0.17 \leq x \leq 0.175$ allowed us to produce a controlled line of acoustic wave delay upon the temperature-controlled phase transition in manganite with $x = 0.175$, operating at near–room temperatures (280–300 K) and controlled by a temperature regulator [11].

ACKNOWLEDGMENTS

This work was supported by the Russian Foundation for Basic Research, project no. 18-08-00203.

REFERENCES

1. Kotani, A., Nakajima, H., Harada, K., and Mori, S., *AIP Adv.*, 2016, vol. 6, p. 056403.
2. Geck, J., Wochner, P., Bruns, D., et al., *Phys. Rev. B*, 2004, vol. 69, p. 104413.
3. Qiu, X., Proffen, Th., Mitchell, J.F., and Billinge, S.J.L., *Phys. Rev. Lett.*, 2005, vol. 94, p. 177203.
4. Sartbaeva, A., Wells, S.A., Thorpe, M.F., et al., *Phys. Rev. Lett.*, 2007, vol. 99, p. 155503.
5. Bulatov, A.R., Bogdanova, Kh.G., Golenishchev-Kutuzov, V.A., Elokhina, L.V., Neifel'd, E.A., and Korolev, A.V., *Phys. Solid State*, 2010, vol. 52, p. 2392.
6. Golenishchev-Kutuzov, V.A., Golenishchev-Kutuzov, A.V., Kalimullin, R.I., and Semennikov, A.V., *J. Low Temp. Phys.*, 2016, vol. 185, p. 558.
7. Darling, T.W., Migliori, A., Moshopoulou, E.G., et al., *Phys. Rev. B*, 1998, vol. 57, p. 5093.
8. Golenishchev-Kutuzov, A.V., Golenishchev-Kutuzov, V.A., Kalimullin, R.I., and Semennikov, A.V., *Phys. Solid State*, 2015, vol. 57, p. 1633.
9. Kotani, A., Nakajima, H., Harada, K., et al., *Phys. Rev. B*, 2016, vol. 94, p. 024407.
10. Asamitsu, A., Moritomo, Y., Kumai, R., et al., *Phys. Rev. B*, 1996, vol. 54, p. 1716.
11. Golenishchev-Kutuzov, A.V., Golenishchev-Kutuzov, V.A., Ismagilov, I.R., Kalimullin, R.I., Potapov, A.A., and Semennikov, A.V., *Tech. Phys. Lett.*, 2014, vol. 40, p. 941.

Translated by L. Mosina

SPELL: 1. ok